Tellus (2004), 56A, 296–307
Printed in UK.

TELLUS

Estimation of bora wind gusts using a limited area model

By DANIJEL BELUŠIĆ* and ZVJEZDANA BENCETIĆ KLAIĆ, *Andrija Mohorovičić Geophysical Institute, Faculty of Science, University of Zagreb, Horvatovac bb, 10000 Zagreb, Croatia*

(Manuscript received 26 June 2003; in final form 23 February 2004)

ABSTRACT

A performance of the wind gust estimate (WGE) method on the bora wind has been examined. Numerical simulations of several bora episodes have been performed using a non-hydrostatic mesoscale model MEMO6. The model captured well the onset and cessation of the bora while the agreement between simulated and observed wind speeds differed from episode to episode. In cases with accurately simulated wind speeds, the WGE results were very good, thus indicating that the method could be used in forecasting bora gusts.

The performance of the WGE method for the examined bora cases also suggested a possibility of further simplification of the method for the bora applications. Inspection of the bora flow and its thermodynamical structure revealed that after the bora onset the shear instabilities completely overwhelm the buoyant forces. This means that the parcels with the maximum wind speed in the boundary layer will always be able to reach the surface and result in wind gusts. Therefore, it is enough to have only a vertical profile of the wind speed. Although completely derived from the physical considerations, this represents a very simple way of determining bora wind gusts and can thus be easily implemented in the operational bora wind forecasting models.

1. Introduction

The bora is a well-known, strong and gusty downslope wind blowing over the eastern Adriatic coast. During the severe bora cases mean hourly wind speed exceeds 17 m s^{-1} (Ivančan-Picek and Tutiš, 1996) and gusts may reach values larger than 50 m s^{-1}. Because of its severity and very frequent occurrence at certain locations (the town of Senj, for example, has annually 177 d with the bora), the bora substantially influences the way of life of local people. Particularly important are the bora gusts which affect traffic, especially over bridges. Therefore, the bridges (such as Maslenica, Pag or Krk) are frequently closed during the strong bora, not only because of the high mean wind speed, but primarily because of the severe wind gusts. It is therefore of the utmost importance to accurately forecast the strength of the bora gusts. In addition, the Adriatic Sea responds in a complex way to the bora forcing (Orlić et al., 1994; Beg Paklar et al., 2001), and there are some indications that the small-scale gust structure might play an important role in the response.

So far, there have been many studies dealing with both theoretical (e.g. Klemp and Durran, 1987; Glasnović and Jurčec, 1990; Enger and Grisogono, 1998) and observational (e.g. Jurčec, 1981; Smith, 1987; Ivančan-Picek and Tutiš, 1995, 1996) aspects of the bora flow. Nevertheless, until recently there were no realistic three-dimensional numerical simulations (Lazić and Tošić, 1998; Tošić and Lazić, 1998; Qian and Giraud, 2000) which could provide a more detailed insight into the flow structure. Therefore, it is hard to expect that there could be any knowledge of the gust dynamics based on the modeling experience, although several attempts have been made to theoretically describe gust formation and structure (Petkovšek, 1982, 1987).

Recently, Brasseur (2001) proposed a new method, fully based on physical approach, for the determination of wind gusts using numerical model results. The new wind gust estimate (WGE) method gave satisfactory results for two explosive cyclogenesis events that resulted in strong wind gusts over Belgium and proved its accuracy for high wind speeds, which makes it potentially applicable to the bora.

In this paper we shall inspect certain characteristics of the bora wind gusts using the WGE method and a mesoscale model MEMO6. We will also propose a modification of the WGE method in order to obtain a new, simpler way of determination of the strength of the bora gusts.

2. Wind gust estimate method

A detailed description of the method can be found in Brasseur (2001). Here we only briefly explain its most important features.

*Corresponding author.
e-mail: dbelusic@rudjer.irb.hr

2.1. Gust estimate

Gusts at the surface are considered to originate from air parcels flowing at higher levels in the boundary layer, which are deflected downward. The mechanism causing the deflection is ascribed to turbulent eddies. It is assumed that if the turbulent eddies have sufficiently large mean turbulent kinetic energy (TKE) to overcome buoyant forces between the surface and a given height, the parcel flowing at that height will be able to reach the surface and produce gusts. This can be summarized with the following relation

$$\frac{1}{z_\mathrm{p}}\int_0^{z_\mathrm{p}} E(z)\,\mathrm{d}z \geq \int_0^{z_\mathrm{p}} g\frac{\Delta\Theta_\mathrm{v}(z)}{\Theta_\mathrm{v}(z)}\,\mathrm{d}z, \qquad (1)$$

where z_p is the height of the given parcel, g is gravity acceleration, Θ_v is the virtual potential temperature, and $\Delta\Theta_\mathrm{v}$ is the variation of virtual potential temperature over a given layer. Because $E(z)$ is the local TKE, the left-hand side of eq. (1) corresponds to the mean TKE in a given layer. The relation may be regarded as formally similar to that of the convective available potential energy. It should be noted that z_p has to be less than the boundary layer height z_top.

Finally, there are many parcels satisfying eq. (1), i.e. the mean TKE is larger than buoyancy at several heights z_p. Hence, the wind gust is estimated as the maximum wind speed among all of those parcels (i.e. heights z_p):

$$Wg_\mathrm{estimate} = \max\left[\sqrt{U^2(z_\mathrm{p}) + V^2(z_\mathrm{p})}\right] \quad \text{for all } z_\mathrm{p} \text{ satisfying eq. (1).} \qquad (2)$$

According to Brasseur (2001), four categories of errors have to be taken into account when using the WGE method: local variability, accuracy of measurements, computed meteorological fields, and limits of the WGE method itself. Therefore, it seems desirable to find a bounding interval around the estimate that should contain the observed gust with a high probability. This additionally requires the determination of lower and upper bounds.

2.2. Lower bound

The lower bound is determined using the same approach as in the gust estimate, only this time it is assumed that the local vertical TKE (instead of the mean for the estimate) is responsible for the deflection of air parcels. The local vertical TKE is given by the vertical velocity variance $\overline{w'w'}(z_\mathrm{p})$, which cannot be obtained from the numerical model used. Therefore, it is calculated diagnostically from the local TKE, $E(z_\mathrm{p})$. This is summarized in the following relation:

$$\frac{\overline{w'w'}(z_\mathrm{p})}{2} = kE(z_\mathrm{p}) \geq \int_0^{z_\mathrm{p}} g\frac{\Delta\Theta_\mathrm{v}(z)}{\Theta_\mathrm{v}(z)}\,\mathrm{d}z. \qquad (3)$$

Here, k denotes a fraction of the local TKE which is attributed to the vertical variance. Brasseur (2001) states that it can vary between the value of $1.7/12.5$ in the surface layer and $1/3$ when the turbulence is closely isotropic in mixed layers. The tests we conducted showed that the results for the bora flow are rather insensitive to changes of k. Therefore, for simplicity we chose the value of $1/3$. Also, the structure of the bora turbulence is not well known but we assume that it may be isotropic, at least in part due to the well-mixed wave-breaking region. This, however, remains a rather unresolved issue (e.g. Smith, 1987).

As in the gust estimate, except that the heights z_p have to satisfy eq. (3), the lower bound is given by

$$Wg_\mathrm{lower} = \max\left[\sqrt{U^2(z_\mathrm{p}) + V^2(z_\mathrm{p})}\right] \quad \text{for all } z_\mathrm{p} \text{ satisfying eq. (3).} \qquad (4)$$

As stated in Brasseur (2001), the estimate is necessarily greater than the lower bound. We shall see later that this does not always apply to the bora flow, where the lower bound is sometimes the same as the estimate.

2.3. Upper bound

Apart from sporadic cases (such as jet streams, deep convections, etc.), it may be presumed that there is no significant turbulence in the free atmosphere. Therefore, it is expected that the maximum wind speed reaching the surface originates from the boundary layer. This assumption is then used in the determination of the upper bound:

$$Wg_\mathrm{upper} = \max\left[\sqrt{U^2(z_\mathrm{p}) + V^2(z_\mathrm{p})}\right] \text{ for all } z_\mathrm{p} \leq z_\mathrm{top}. \qquad (5)$$

The boundary layer height z_top is often determined as the height where the TKE reaches 1% of its surface value (Brasseur, 2001). However, due to the bora specific dynamical structure, both assumptions (the non-turbulent free atmosphere and the boundary layer height being a fraction of the surface TKE) will have to be reconsidered. This issue will be discussed in the following sections.

The advantage of the WGE method lies in the fact that it is entirely based on physical considerations. It is, however, highly sensitive to the accuracy of the modeled meteorological fields. This should be kept in mind when the results are being evaluated.

3. Observational data

The surface wind speed measurements are used for the comparison with the results of the numerical model (see the next section). The measured wind speeds correspond to the hourly means, except for Krk and Maslenica where the means are determined from the 10-min intervals. The hourly wind gusts correspond to the maximum measured wind speeds within the hour.

The anemometers at Senj and Zadar are positioned at 10 m above ground, while those at Krk and Maslenica are at 3 m. Because the lowest level in the model is 10 m, the wind speeds have been interpolated to 3 m at Krk and Maslenica using a log wind profile with the roughness length value of 0.03 m. The value of 0.03 m has been proposed by the staff of the Meteorological and Hydrological Service of Croatia because at both locations the anemometers are positioned at bridges over the sea, and thus roughness length values are smaller than over the ground. This value may also be considered, in a loose manner, as a sort of medium value (in logarithmic sense) between the water and the mountainous terrain. The interpolation has been performed only for the comparison with the hourly mean wind speeds. It is not required for the wind gusts, due to their non-local character (Brasseur, 2001).

4. Numerical simulations

This section is devoted to the presentation of the numerical model performance and accuracy for several bora cases. This is important because the simulated meteorological fields will be used later as the input for the WGE method, which is, as mentioned earlier, highly dependent on the model accuracy.

4.1. Numerical model

A three-dimensional non-linear non-hydrostatic prognostic mesoscale model for unsaturated air (MEMO, version 6.0) is employed. A detailed model description and its performance have been documented in previous publications (Moussiopoulos, 1995; Caballero and Lavagnini, 2002; Klaić and Nitis, 2002; Klaić et al., 2002, 2003a) and here we provide only a brief overview. The model vertical coordinate is terrain following. The model solves the continuity equation, momentum equations, and prognostic equations for scalars (potential temperature, specific humidity and TKE). The equations are solved using finite differences on a staggered Arakawa C grid. The temporal discretization of the equations is based on the second-order Adams–Bashforth scheme, except for the non-hydrostatic part of the mesoscale pressure perturbation (which is treated implicitly) and the vertical turbulent diffusion (where the second-order Crank–Nicholson method is used). The advection scheme is the second-order total-variation-diminishing scheme (Harten, 1986).

The model is initialized using an objective analysis model (Moussiopoulos and Flassak, 1989). The input fields are updated at the periods when the soundings are available. At all lateral boundaries, expanded radiation conditions are used (Carpenter, 1982) to allow not only the propagation of the disturbances out of the domain through the boundary, but also for the information from outside to be imposed at the boundary. For the non-hydrostatic part of the mesoscale pressure perturbation, homogeneous Neumann boundary conditions are used at lateral boundaries. This ensures that the wind velocity component perpendicular to the boundary remains unaffected by the pressure change.

The lower boundary almost coincides with the ground, where for the non-hydrostatic part of the mesoscale pressure perturbation, inhomogeneous Neumann conditions are imposed ('no-flow-through' boundary). All other conditions at the lower boundary follow from the assumption that the Monin–Obukhov similarity theory is valid.

At the upper boundary, Neumann boundary conditions are imposed for the horizontal velocity components and the potential temperature. To ensure non-reflectivity, the radiative condition is used for the hydrostatic part of the mesoscale pressure perturbation at that boundary. Hence, vertically propagating internal gravity waves are allowed to leave the computational domain (Klemp and Durran, 1983). For the non-hydrostatic part of the mesoscale pressure perturbation, homogeneous Dirichlet conditions are imposed because of negligible non-hydrostatic effects at large heights.

4.2. Simulation of bora episodes

All cases were simulated using a unique three-dimensional domain at the horizontal resolution of 3 km and the time increment of 10 s. High resolution is essential in obtaining satisfactory results from the simulations in complex terrain (Cairns and Corey, 2003). The center of the 300×300 km^2 domain was placed on 45°N, 15°E. The model top was set at 10 000 m above the surface. In the vertical, 30 layers were selected with a finer resolution at lower altitudes. Layer depths gradually increased from 20 m at the bottom to approximately 1400 m at the top of the modeling domain.

The model was driven with the Zagreb–Maksimir (45.82°N, 16.03°E, 128-m ASL) radiosonde data. This is adequate for most bora cases because there is usually a strong north-easterly pressure gradient between the continental parts of Croatia (namely Zagreb, which is located north-east of Adriatic coast) and the coast. This results in the fact that the upstream bora flow, i.e. the flow incident on the mountain barrier, does not change the characteristics represented by Zagreb soundings significantly before it reaches the mountain. Moreover, the main processes leading to the severe wind state take place in the lee of the mountain. Therefore, the upstream conditions provide the necessary environment for the transition to the severe state. However, once the bora starts, its behavior depends mainly on the small-scale features in the topography. This is also why fine horizontal resolution was employed in the simulations.

Figure 1 shows the modeling domain, together with the comparison between the simulated and measured vertical profiles of potential temperature, wind speed and direction at Zagreb–Maksimir at 12 UTC 7 November 1999 (the MAP bora; see the following paragraph). The comparison is shown to confirm the ability of the model to accurately reproduce the upwind thermodynamical structure.

Several periods of the bora were chosen. The first bora period, 5–8 November 1999, coincided with the Mesoscale Alpine Programme (MAP) Intensive Observation Period (IOP) 15 (6–7 November 1999). Therefore, Zagreb soundings were more frequent (every 3 h) compared to the standard 00 and 12 UTC

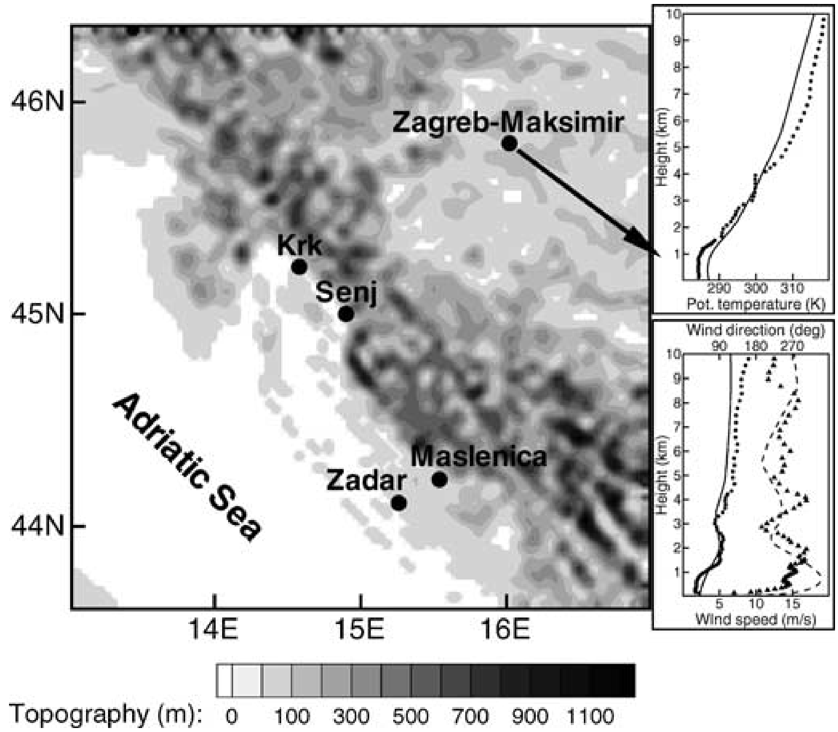

Fig 1. Modeling domain (300 × 300 km^2) with locations of the wind speed measuring sites and Zagreb–Maksimir radiosonde station. The two panels on the right show the comparison between the simulated and sounded vertical profiles of potential temperature (upper panel: solid line, simulated; circles, measured), wind direction (lower panel: solid line, simulated; circles, measured) and wind speed (lower panel: dashed line, simulated; triangles, measured) over Zagreb–Maksimir on 12 UTC 7 November 1999.

observations. Thus, better forcing at the boundaries was provided. Other simulations were conducted during December 2001 and January 2002 when an additional anemometer was installed at Senj at a different location. Comparison between the wind speeds recorded by the standard anemometer at Senj and the additionally installed one revealed that the standard anemometer underestimates strong north-easterly winds due to its sheltered position relative to the bora. Thus, we may expect that the additional anemometer will be more representative for the bora. Nevertheless, available measurements of both anemometers will be shown here. One should keep in mind that our main goal is to obtain good agreement in order to provide as accurate as possible input for the WGE method. Consequently, for each episode we will consider the data of the anemometer that agree better with the model as representative.

Because the bora exhibits very complicated temporal and spatial behavior, different parts of the coast may not simultaneously be under the same conditions. It is, therefore, possible that the bora appears in the southern part of the model domain (e.g. Maslenica) a few days after the onset in the northern part (e.g. Krk). Furthermore, high winds sometimes occur only in a narrow region in the lee of the mountain (e.g. Senj) while all other parts have different conditions. Therefore, only results for the stations with severe wind will be shown. Time units are given in local standard time (LST) which is an hour ahead of UTC.

4.2.1. Mesoscale Alpine Programme period. Figure 2 shows a comparison between the simulated and observed hourly wind speeds at Krk, Senj and Maslenica from 12 LST 6 November to 23 LST 8 November 1999. The model accurately captured the onset of the bora at all three stations. The simulated and observed wind speeds are rather well correlated for Krk and Maslenica, although underestimated by the model, except for the period from hour 20 to hour 28 of the simulation for Krk. This can be attributed to the local effects that cannot be resolved by the model resolution employed. On the other hand, the simulated wind speeds at Senj seem to be highly overestimated. However, this could be attributed to the already mentioned underestimation of the bora wind speed by the standard anemometer at Senj.

4.2.2. 13–16 December 2001. Figure 3 shows the comparison at Krk, Senj, Maslenica and Zadar from 00 LST 13 December to 13 LST 16 December 2001. Hour-to-hour variations at Krk are not well simulated, but the onset and main variation are acceptable. During the episode, the model underestimated the wind speeds. Agreement is much better at Senj (standard anemometer data), apart from hour 42 to hour 70 of the simulation. During that period (over a day long), the local channeling effects at Senj caused the persistence of the bora although it became diminished at all other locations. This situation is very frequent at Senj when the bora is concerned. To accurately simulate these mechanisms, a domain at much finer resolution (a few hundred meters) should be used, which is beyond our current abilities. At Maslenica, the simulated wind speeds are highly underestimated. However, the main variation that is present at all stations except Senj is well captured. The time of the onset is also accurately simulated. The bora at Zadar was not as severe. At this site the simulated and observed values agree well.

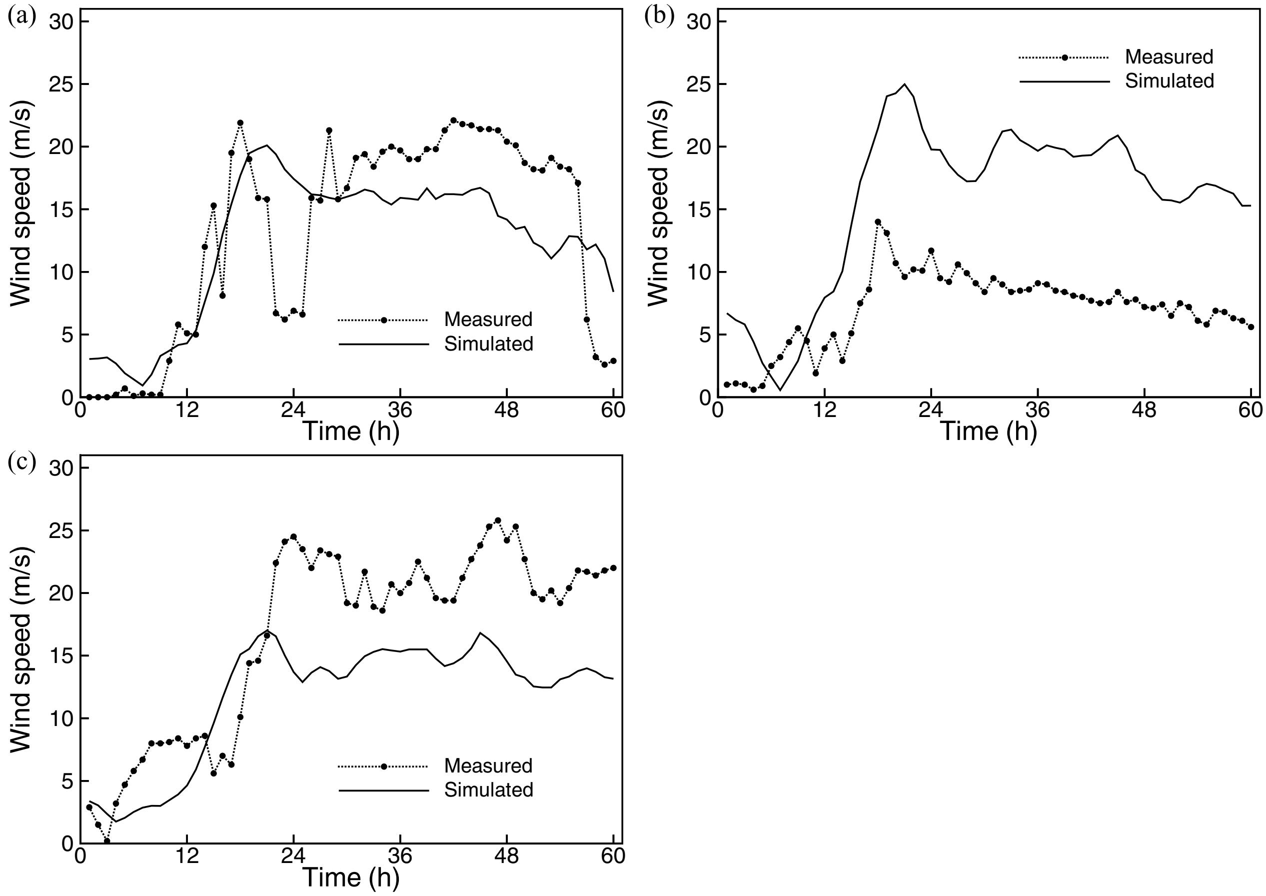

Fig 2. A comparison between observed and simulated hourly wind speeds at (a) Krk, (b) Senj and (c) Maslenica from 12 LST 6 November to 23 LST 8 November 1999.

4.2.3. 29–31 December 2001. During this period (00 LST 29 December to 23 LST 31 December 2001) the bora was accurately simulated only at Senj (Fig. 4). The part of the time series without the bora (approximately the first 30 h of the simulated period) is shown here because the wind speeds were high enough so that the inspection of the performance of the WGE method under the non-bora conditions could be provided. It is important for the wind speed to be sufficiently high because Brasseur (2001) found that the WGE method is most reliable for gusts above 10 m s^{-1}. Here, the agreement is much better with the additional anemometer. The standard anemometer measurements were available starting at hour 18 of the simulation.

4.2.4. 13–18 January 2002. This period is characterized with the bora appearing only over the northern Adriatic. For this reason, only Krk and Senj are shown in Fig. 5. The simulation was performed from 00 LST 13 January to 23 LST 18 January 2002. The simulated and observed values agree well, especially for Krk. Senj is again influenced by the local effects, which generally result in the occurrence of the bora even if it does not exist anywhere else. This is most obvious during the first 15 h of the simulation. The model showed very low wind speeds (below 5 m s^{-1}), similarly to the situation at Krk, while the observed values were between 10 and 15 m s^{-1}. The standard anemometer was available only in the second part of the period (beginning at hour 85 of the simulation).

All the results presented here, although not perfect, are satisfactory considering the known difficulties with modeling of the bora-type winds.

5. Bora gust estimates

In this section we present results of the application of the WGE method to the bora wind. The periods inspected here coincide with those from the previous section.

The method requires the determination of the boundary layer height, which is often calculated as $E_{\mathrm{top}} = 0.01 E_{\mathrm{surface}}$ (Brasseur, 2001), where E_{top} and E_{surface} are the values of the TKE at the top of the boundary layer and at the surface, respectively. The vertical profile of the TKE during the bora has a rather complicated structure due to the appearance of an additional maximum at heights well above 500 m (cf. Fig. 10). The structure is typical for downslope windstorms where the upper TKE

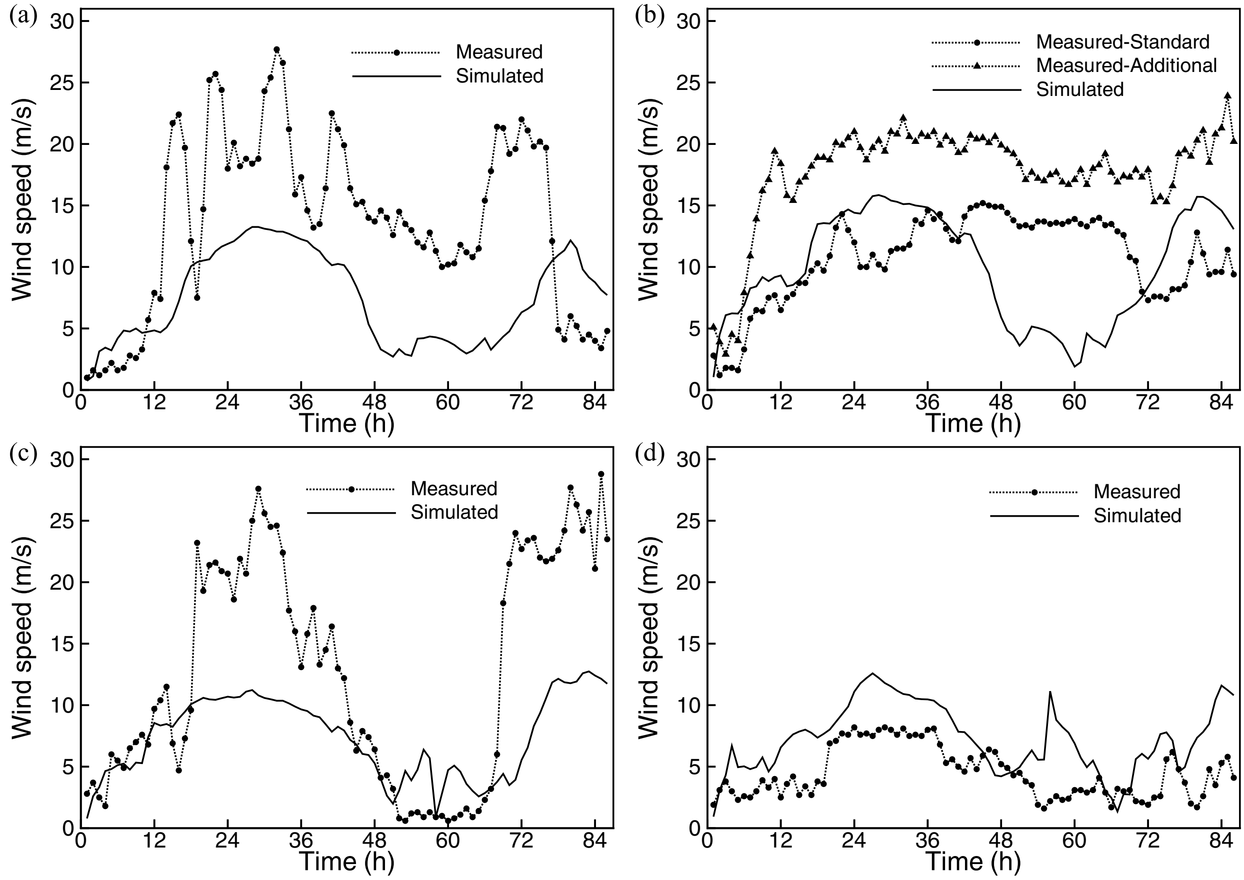

Fig 3. A comparison between observed and simulated hourly wind speeds at (a) Krk, (b) Senj, (c) Maslenica and (d) Zadar from 00 LST 13 December to 13 LST 16 December 2001.

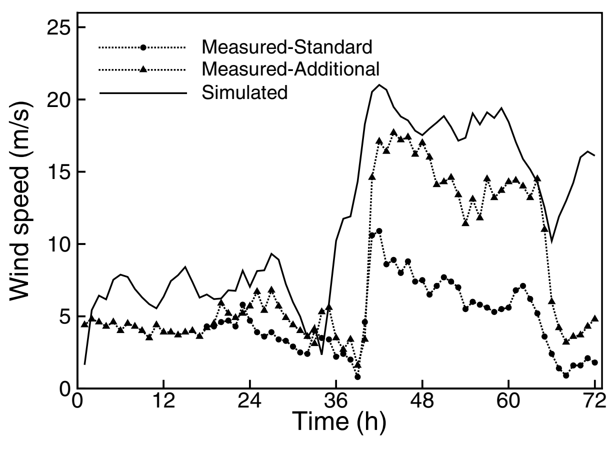

Fig 4. A comparison between observed and simulated hourly wind speeds at Senj from 00 LST 29 December to 23 LST 31 December 2001.

maximum is associated with the wave-breaking region (Enger and Grisogono, 1998; Klaić et al., 2003b). This, however, complicates the determination of the boundary layer height. Thus, a slight simplification in the determination of the boundary layer height has been adopted here: the boundary layer height is replaced with the bora layer height after the bora onset. The bora layer height in the lee of the mountain is defined as a layer capped with the critical level (defined for the mountain waves as the level where the cross-mountain component of the wind speed disappears). The atmosphere above the bora layer is considered as undisturbed by the bora flow. This matter will also be referred to in the next section.

Table 1 shows measured and simulated hourly wind speeds and gusts averaged over the simulated periods. In most cases the model underestimates the mean wind speed, which then reflects to the gust estimate. Thus, it is generally the case (except at Krk during the MAP period, where the differences between the simulated and measured data are rather small) that when the mean wind speeds are underestimated, the gusts are underestimated too; also, when the mean wind speeds are overestimated, so are the gusts. This confirms the claim that the accuracy of the WGE method is highly dependent on the simulated fields, but it is also clear that there is a strong positive correlation between the bias in the simulated wind speeds and the estimated wind gusts. A detailed inspection of the particular periods follows.

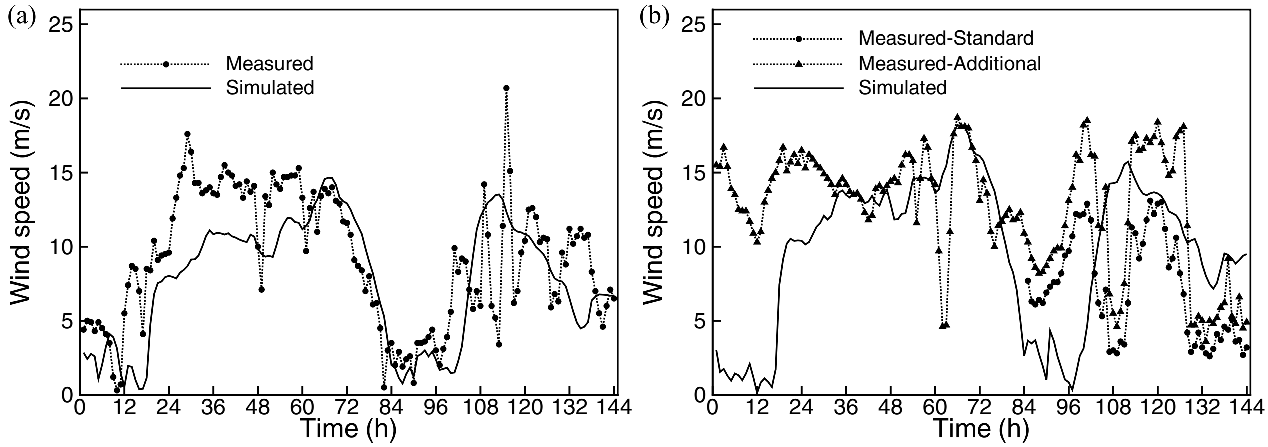

Fig 5. A comparison between observed and simulated hourly wind speeds at (a) Krk and (b) Senj from 00 LST 13 January to 23 LST 18 January 2002.

Table 1. Wind speeds and gusts averaged over the simulated bora episodes.

		Wind speed (m s^{-1})		Wind gust (m s^{-1})	
Period	Location	Simulated	Measured	Simulated	Measured
12 LST 6 Nov to 23 LST 8 Nov 1999	Krk	12.4	13.1	25.0	22.3
	Senj	15.7	7.1	24.8	18.1
	Maslenica	11.8	16.7	23.4	30.4
	Zadar	–	–	–	–
00 LST 13 Dec to 13 LST 16 Dec 2001	Krk	7.5	13.7	14.3	28.6
	Senj	9.9	10.8	14.4	23.6
	Maslenica	7.5	12.8	13.8	25.5
	Zadar	7.3	4.5	10.7	9.6
00 LST 29 Dec to 23 LST 31 Dec 2001	Krk	–	–	–	–
	Senj	11.7	7.9	18.6	17.8
	Maslenica	–	–	–	–
	Zadar	–	–	–	–
00 UTC 13 Jan to 23 UTC 18 Jan 2002	Krk	7.7	9.2	13.7	20.0
	Senj	9.8	12.7	13.3	26.1
	Maslenica	–	–	–	–
	Zadar	–	–	–	–

5.1. Mesoscale Alpine Programme period

The results of the WGE method are shown in Fig. 6. When compared with the results for the mean wind speed from the previous section (Fig. 2), it is obvious that the WGE method gives as accurate a gust estimate as the simulated wind speeds are. Hence, the agreement for Krk is very good except between hours 20 and 28 of the simulation. For Senj, the calculated gusts are overestimated, while for Maslenica they are slightly underestimated. These results are encouraging because they imply an accurate prediction of the wind gusts if accurate input fields are provided. When the bora is concerned, this primarily means that wind gust estimates will become substantially more accurate if a high enough resolution is employed in the wind speed simulations (e.g. Tudor and Ivatek-Šahdan, 2002). It should be noted that, at many points during the bora, the lower bound, gust estimate and upper bound merge into a single value, turning the bounding interval around the gust estimate to zero. In such situations, the gust is equal to the maximum wind speed in the boundary layer. This is found to be typical for the bora.

5.2. 13–16 December 2001

This case also confirms the postulation that the WGE method is as accurate as the simulated meteorological fields. Thus, as seen in Fig. 7, gust estimates at Krk and Maslenica are highly underestimated exactly at the points where the simulated wind speeds are lower than those observed (see Fig. 3). The main wave-like pattern of the time series (i.e. maximum around hours 24 and 84 and minimum around hour 60 of the simulation) is well represented. The agreement for Senj is very good at the points

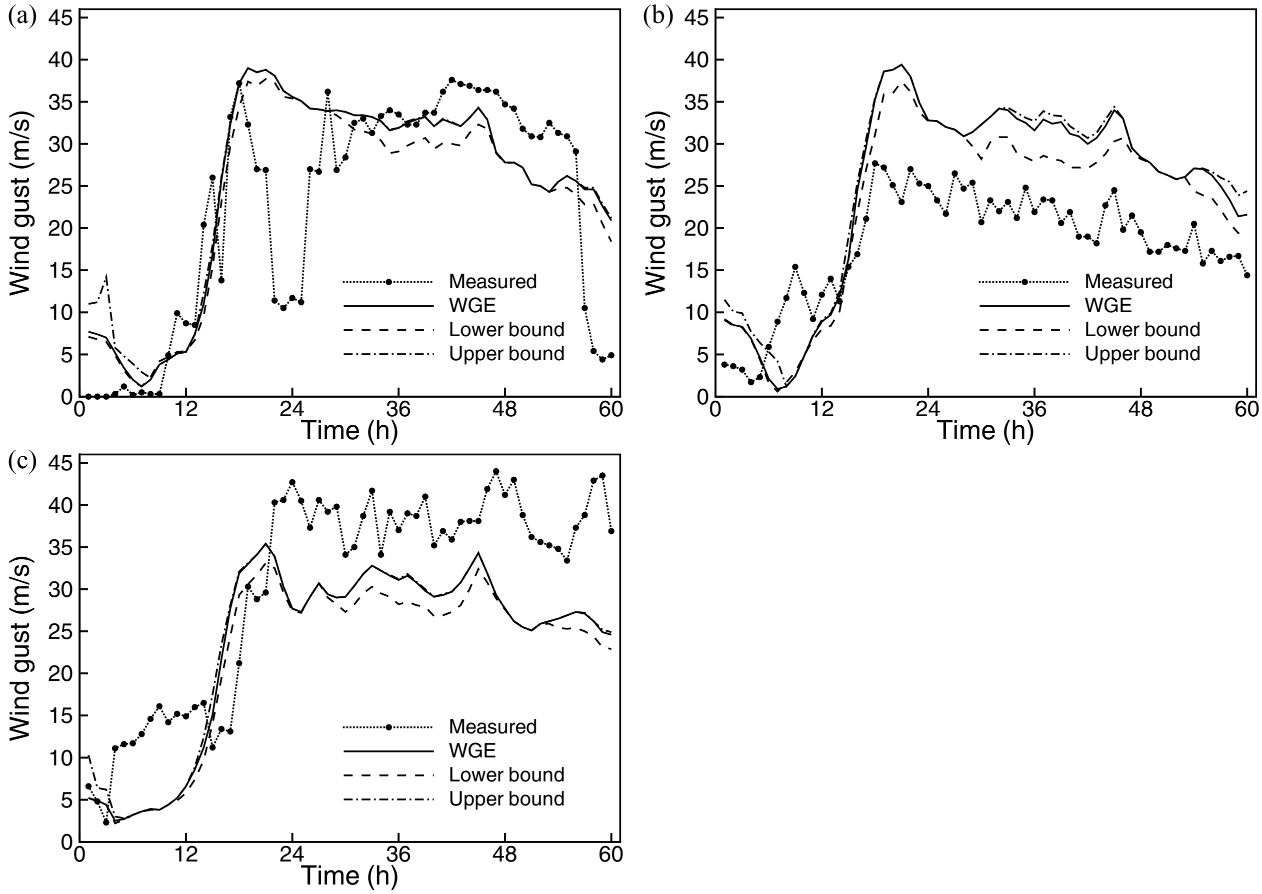

Fig 6. A comparison between simulated (wind gust estimate, lower and upper bound) and observed hourly wind gusts at (a) Krk, (b) Senj and (c) Maslenica from 12 LST 6 November to 23 LST 8 November 1999. Compare with Fig. 2.

where the model successfully simulated the bora. However, as noted earlier, between hours 42 and 70 of the simulation the model did not capture the bora flow and thus the gust estimates are unsatisfactory for that period. Good agreement at Zadar was expected, partly because the wind speeds and gusts were much lower there, and the model underestimated these quantities at surrounding stations which were under severe bora conditions.

5.3. 29–31 December 2001

As seen in Fig. 8, this case can be divided into two periods: the first 36 h characterized with the non-bora conditions and the last 36 h with the bora. These periods are selected in order to clearly demonstrate how severely the atmospheric conditions change after the bora onset, yielding the gust estimate, the upper bound and, in some cases, the lower bound to overlap. This merging can also be observed in all other bora episodes, except that in hours without the bora the wind speeds and gusts were very low there, and thus the bounding interval around the gust estimate remained rather small even without the presence of the bora flow. On the other hand, Brasseur (2001) obtained generally larger bounding intervals. In this study, larger bounding intervals exist only in this particular case, because the wind speeds during the first period were sufficiently high. Nevertheless, the fact that the interval almost disappears during the bora is of much greater importance here. A thorough explanation of this phenomenon will be provided in the next section.

5.4. 13–18 January 2002

Figure 9 shows that the method underestimated the gusts. Because the upper bound and gust estimate almost coincide, and bearing in mind that the upper bound is the maximum wind speed in the boundary layer, it can be concluded that the model systematically underestimated the boundary layer wind speeds. This is particularly evident at Senj. Because this station is highly influenced by the local effects, it is presumed that the underestimation is due to the too coarse resolution of the domain. However, the agreement at Krk is much better and the general temporal variation is very well captured.

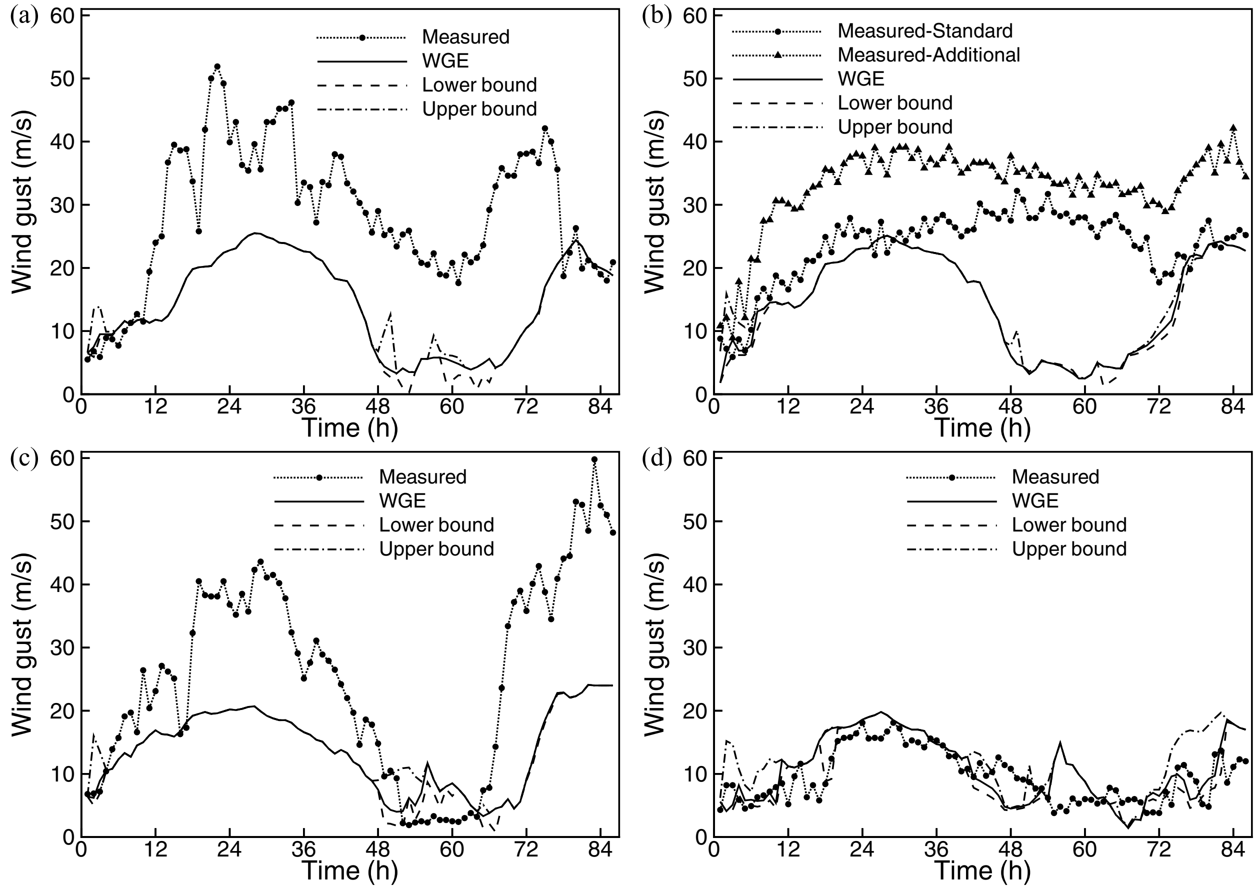

Fig 7. A comparison between simulated (wind gust estimate, lower and upper bound) and observed hourly wind gusts at (a) Krk, (b) Senj, (c) Maslenica and (d) Zadar from 00 LST 13 December to 13 LST 16 December 2001. Compare with Fig. 3.

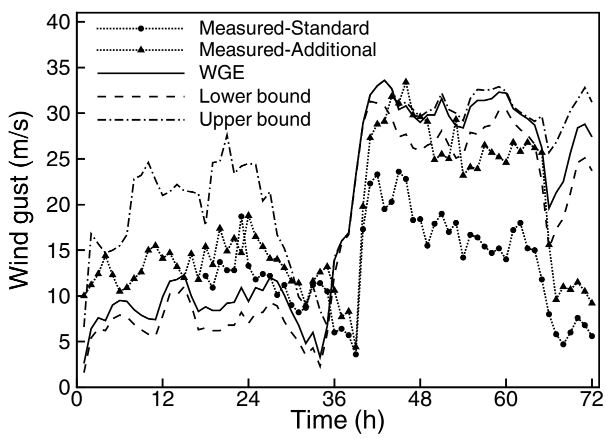

Fig 8. A comparison between simulated (wind gust estimate, lower and upper bound) and observed hourly wind gusts at Senj from 00 LST 29 December to 23 LST 31 December 2001. Compare with Fig. 4.

6. Discussion

The results shown here confirm the ability of the numerical model to reproduce the bora wind gusts, provided that the mean wind speeds are accurately simulated. This may have a great influence on forecasting of the bora wind gusts. Additionally, in order to make the gust estimating procedure as simple as possible and without losing any relevant information about the gust behavior, certain modifications of the WGE method will be proposed.

Because the bora has many dynamical similarities with downslope winds in other parts of the world (namely the Boulder windstorm; Smith, 1987), and gustiness is one of them, it is appropriate to extend some of the results obtained in the numerical studies of those phenomena to the bora flow. In a series of papers, Scinocca and Peltier (Scinocca and Peltier, 1989, 1993, 1994; Peltier and Scinocca, 1990), using idealized numerical simulations, proposed a Kelvin–Helmholtz (K–H) instability as the mechanism responsible for the gust generation. This was confirmed by the study of Wang and Lin (1999), while Smith (1991) obtained similar results using a theoretical approach. The K–H instability is a dynamical instability and it appears only in enhanced shear zones. Because the simulations of Scinocca and Peltier did not include surface friction, the maximum wind speed was located near the surface. Hence, the shear region responsible for the gusts was located above the maximum wind speed. However, when the

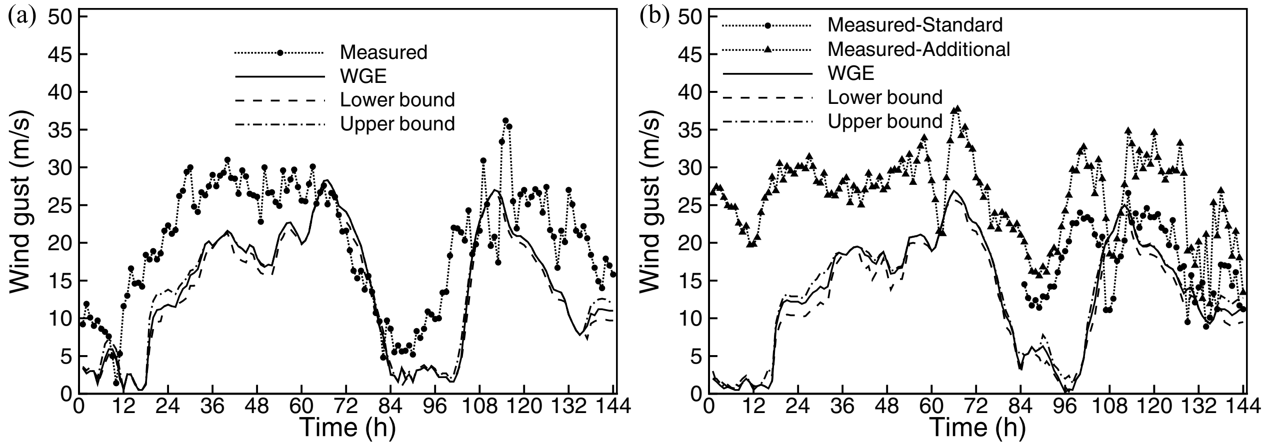

Fig 9. A comparison between simulated (wind gust estimate, lower and upper bound) and observed hourly wind gusts at (a) Krk and (b) Senj from 00 LST 13 January to 23 LST 18 January 2002. Compare with Fig. 5.

surface friction is included in the model, the wind speed reaches its maximum at a certain height above the surface. This results in the appearance of another shear zone that is positioned between the ground and the maximum wind speed height. Figure 10 shows vertical profiles of the TKE and gradient Richardson number (*Ri*) averaged over all bora episodes at Krk

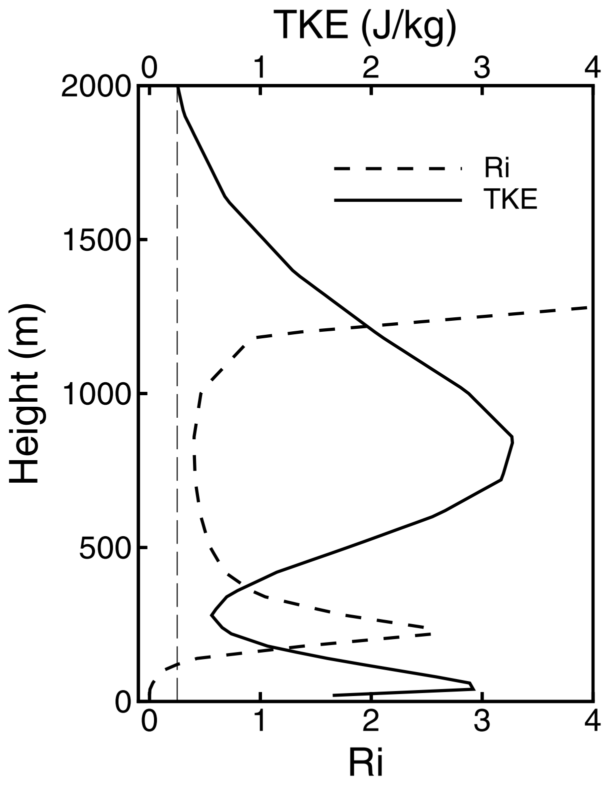

Fig 10. Vertical profiles of the gradient Richardson number and TKE at Krk averaged over all bora episodes during January 2002. Dashed vertical line represents a boundary ($Ri = 0.25$) below which the K–H instability appears.

during January 2002 and represents the typical vertical bora structure. The TKE values are between the values published in the previous studies, which ranged from 1 $m^2\ s^{-2}$ in three-dimensional numerical studies (e.g. Qian and Giraud, 2000) to of the order of 10 $m^2\ s^{-2}$, obtained from aircraft measurements (Smith, 1987). The levels with the minimum *Ri* correspond to the levels with the maximum TKE, while the height where the *Ri* reaches its low-level maximum (225 m) corresponds to the maximum wind speed height (cf. Fig. 11). Because low *Ri* indicates dynamically unstable regions resulting from enhanced shear, several conclusions can be drawn. First of all, static stability will only have a minor influence on the production or destruction of the TKE, meaning that the main mechanism of the TKE production will be of dynamical (shear) origin. Also, bearing in mind that the K–H instability will appear when $Ri < Ri_{\mathrm{critical}} = 0.25$, it is evident that the TKE (which is one of the key variables in the WGE method) within the layer between the ground and the height of the maximum wind speed will be produced by the K–H instability. As the value of 0.25 for Ri_{critical} is determined theoretically for idealized conditions, it may well be that the value of 0.4, which is the upper-level minimum of *Ri* (at 850 m), is less than Ri_{critical} for complex-terrain situations with non-parallel flow. This is additionally substantiated by the fact that the TKE profile is also strongly dependent on *Ri* at those heights (roughly 500–1000 m), and is therefore possibly of K–H origin as well. Furthermore, all of the above yields that the TKE profiles will be similar in all bora cases because the wind speed profiles are similar by the very nature of the bora. The last statement leads us to the possibility of simplification of the WGE method for the bora wind applications.

Figure 11 shows vertical profiles of all variables used in the WGE method averaged over January 2002 bora episodes at Krk as in Fig. 10. The upper horizontal line indicates the height below which the mean TKE is greater than the buoyant energy. According to the method, in that layer (i.e. between the ground and the upper line) air parcels may be deflected toward the

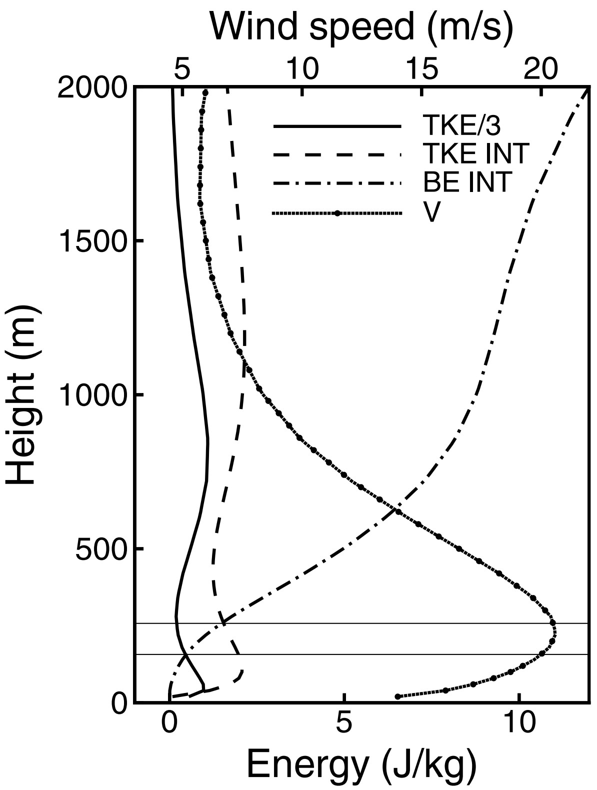

Fig 11. Vertical profiles of 1/3 TKE (corresponding to the local vertical TKE), mean TKE in a given layer (TKE INT), buoyant energy (BE INT) and wind speed (V) at Krk averaged over all bora episodes during January 2002. The two horizontal lines mark the upper limits of the lower bound and gust estimate (see text for further details).

ground. As each deflected parcel carries different momentum (i.e. different wind speed), depending on the original parcel height, the gust estimate will simply be the maximum wind speed within the specified layer. Similarly, the lower bound of the bounding interval (see Section 2) will be the maximum wind speed below the lower line, i.e. the maximum wind speed within the layer where the local vertical TKE is greater than the buoyant energy. Finally, the upper bound will be the maximum wind speed in the boundary (bora) layer. It is evident from the figure that the upper line is located above the height of the maximum wind speed. This means that the gust estimate will generally be equal to the upper bound. The lower line is slightly below the maximum wind speed, thus indicating that the lower bound will generally be slightly smaller than the gust estimate and upper bound. However, because Fig. 11 shows averaged profiles it is very likely that the lower bound will occasionally also become equal to the upper bound (e.g. Fig. 6). This is evident if the time series of all bora cases are inspected. In addition, it can be seen that it is completely irrelevant how the boundary layer height is determined during the bora as far as it reaches above the maximum wind speed in the layer. This is always fulfilled if the bora layer height is used.

Based on the arguments above, it can be concluded that generally for situations with the bora the complete WGE method can be reduced only to the calculation of the upper bound, i.e. the maximum wind speed in the boundary layer. Thus, there is no need for any consideration of the energetics. This modification substantially simplifies the method and leads to its greater operability.

7. Conclusions

In this study we inspected the possibility of obtaining the bora wind gusts from a mesoscale numerical model. Simulations of several cases of the bora wind have been performed using the mesoscale model MEMO6, while the WGE method has been used for the estimation of the gusts. The model generally underestimates high wind speeds, which is partly due to the nature of the bora wind, which possibly requires very high resolution for accurate simulations. Nevertheless, the temporal variations of the wind speed during the simulated periods are overall very well simulated. Also presented are the results of the application of the WGE method to the bora flow. The estimated gusts agree reasonably well with those observed, especially if the mean wind speeds are accurately simulated. It is also seen that the biases of simulated wind speeds and wind gusts are proportional. This makes the method applicable for the bora gust forecasting.

Additionally, based on the inspection of behavior of the wind gusts and the dynamical structure of the bora flow we found a way to simplify the method: it suffices to find the maximum wind speed in the bora layer and pronounce it the wind gust. This makes the calculation much easier to perform as it does not require any knowledge about the energetics (TKE and buoyant energy profiles). The only data needed are the vertical profiles of the wind speed. Because of the simplicity, the implementation of this procedure within the operational bora wind forecasting models seems plausible and may thus lead to more punctual warnings of the high-wind-gust events.

8. Acknowledgments

We would like to thank the Meteorological and Hydrological Service of the Republic of Croatia for providing observational data. Particular thanks are due to Mr Zvonko Žibrat for his engagement and to M. Sc. Alica Bajić for helpful discussions. This study, together with the additional anemometer measurements, was performed under Project 'Atmosphere-Adriatic System', No. 0119330, sponsored by the Ministry of Science and Technology of the Republic of Croatia.

References

Beg Paklar, G., Isakov, V., Koračin, D., Kourafalou, V. and Orlić, M. 2001. A case study of bora-driven flow and density changes on the Adriatic Shelf (January 1987). *Cont. Shelf Res*. **21**, 1751–1783.

Brasseur, O. 2001. Development and application of a physical approach to estimating wind gusts. *Mon. Wea. Rev*. **129**, 5–25.

Caballero, R. and Lavagnini, A. 2002. A numerical investigation of the sea breeze and slope flows around Rome. *Nouvo Cimento*. **25C**, 287–304.

Cairns, M. M. and Corey, J. 2003. Mesoscale model simulations of high-wind events in the complex terrain of western Nevada. *Weather Forecast*. **18**, 249–263.

Carpenter, K. M. 1982. Note on the paper "Radiation condition for the lateral boundaries of limited area numerical models". *Q. J. R. Meteorol. Soc*. **108**, 717–719.

Enger, L. and Grisogono, B. 1998. The response of bora-type flow to seasurface temperature. *Q. J. R. Meteorol. Soc*. **124**, 1227–1244.

Glasnović, D. and Jurčec, V. 1990. Determination of upstream bora layer depth. *Meteorol. Atmos. Phys*. **43**, 137–144.

Harten, A. 1986. On a large time-step high resolution scheme. *Math. Comp*. **46**, 379–399.

Ivančan-Picek, B. and Tutiš, V. 1995. Mesoscale bora flow and mountain pressure drag. *Meteorol. Z*. **4**, 119–128.

Ivančan-Picek, B. and Tutiš, V. 1996. A case study of a severe Adriatic bora on 28 December 1992. *Tellus*. **44A**, 357–367.

Jurčec, V. 1981. On mesoscale characteristics of bora conditions in Yugoslavia. *Pure Appl. Geophys*. **119**, 640–657.

Klaić, Z. B. and Nitis, T. 2001–2002. Application of mesoscale model (MEMO) to the greater Zagreb area during summertime anticyclonic weather conditions. *Geofizika*. **18–19**, 31–43.

Klaić, Z. B., Nitis, T., Kos, I. and Moussiopoulos, N. 2002. Modification of the local winds due to hypothetical urbanization of the Zagreb surroundings. *Meteorol. Atmos. Phys*. **79**, 1–12.

Klaić, Z. B., Belušić, D., Bulić, I. H. and Hrust, L. 2003a. Mesoscale modeling of meteorological conditions in the lower troposphere during a winter stratospheric ozone intrusion over Zagreb, Croatia. *J. Geophys. Res*. **108**, 4720.

Klaić, Z. B., Belušić, D., Grubišić, V., Gabela, L. and Ćoso, L. 2003b. Mesoscale airflow structure over the northern Croatian coast during MAP IOP 15 – a major Bora event. *Geofizika*. **20**, 23–61.

Klemp, J. B. and Durran, D. R. 1983. An upper boundary condition permitting internal gravity wave radiation in numerical mesoscale models. *Mon. Wea. Rev*. **111**, 430–444.

Klemp, J. B. and Durran, D. R. 1987. Numerical modelling of bora winds. *Meteorol. Atmos. Phys*. **36**, 215–227.

Lazić, L. and Tošić, I. 1998. A real data simulation of the Adriatic bora and the impact of mountain height on bora trajectories. *Meteorol. Atmos. Phys*. **66**, 1–10.

Moussiopoulos, N. 1995. The EUMAC Zooming model, a tool for local-to-regional air quality studies. *Meteorol. Atmos. Phys*. **57**, 115–133.

Moussiopoulos, N. and Flassak, Th. 1989. A diagnostic wind model and its interactions with observations and experiments. In: *Computers and Experiments in Fluid Flow* (eds G. M. Carlomagno, and C. A. Brebbia). Springer-Verlag, Berlin, 239–250.

Orlić, M., Kuzmić, M. and Pasarić, Z. 1994. Response of the Adriatic Sea to the bora and sirocco forcing. *Cont. Shelf Res*. **14**, 91–116.

Peltier, W. R. and Scinocca, J. F. 1990. The origin of severe downslope windstorm pulsations. *J. Atmos. Sci*. **47**, 2853–2870.

Petkovšek, Z. 1982. Gravity waves and bora gusts. *Ann. Meteorol*. **19**, 108–110.

Petkovšek, Z. 1987. Main bora gusts – a model explanation. *Geofizika*. **4**, 41–50.

Qian, M. W. and Giraud, C. 2000. A preliminary numerical simulation of bora wind with a limited area model of atmospheric circulation. *Nouvo Cimento*. **23C**, 515–523.

Scinocca, J. F. and Peltier, W. R. 1989. Pulsating downslope windstorms. *J. Atmos. Sci*. **46**, 2885–2914.

Scinocca, J. F. and Peltier, W. R. 1993. The instability of Long's stationary solution and the evolution toward severe downslope windstorm flow. Part I: nested grid numerical simulations. *J. Atmos. Sci*. **50**, 2245–2263.

Scinocca, J. F. and Peltier, W. R. 1994. The instability of Long's stationary solution and the evolution toward severe downslope windstorm flow. Part II: the application of finite-amplitude local wave-activity flow diagnostics. *J. Atmos. Sci*. **51**, 623–653.

Smith, R. B. 1987. Aerial observations of the Yugoslavian bora. *J. Atmos. Sci*. **44**, 269–297.

Smith, R. B. 1991. Kelvin–Helmholtz instability in severe downslope wind flow. *J. Atmos. Sci*. **48**, 1319–1324.

Tošić, I. and Lazić, L. 1998. Improved bora wind simulation using a nested Eta Model. *Meteorol. Atmos. Phys*. **66**, 143–155.

Tudor, M. and Ivatek-Šahdan, S. 2002. MAP IOP 15 case study. *Croat. Meteorol. J*. **37**, 1–14.

Wang, T.-A. and Lin, Y.-L. 1999. Wave ducting in a stratified shear flow over a two-dimensional mountain. Part II: implications for the development of high-drag states for severe downslope windstorms. *J. Atmos. Sci*. **56**, 437–452.